Understanding the unusual friction behavior of hydrogen-free diamond-like carbon films in oxygen atmosphere by first-principles calculations

Liping Wang [a, c, *], Longchen Cui [b, c], Zhibin Lu [c], Hui Zhou [b]

[a] Key Laboratory of Marine Materials and Related Technologies, Zhejiang Key Laboratory of Marine Materials and Protective Technologies, Ningbo Institute of Materials Technology and Engineering, Chinese Academy of Sciences, Ningbo 315201, China
[b] Science and Technology on Vacuum Technology and Physics Laboratory, Lanzhou Institute of Physics, Lanzhou 730000, China
[c] State Key Laboratory of Solid Lubrication, Lanzhou Institute of Chemical Physics, Chinese Academy of Sciences, Lanzhou 730000, China

ARTICLE INFO

Article history:

ABSTRACT

The friction coefficients of diamond and hydrogen-free diamond-like carbon films were reported to be in an intermediate range, from 0.2 to 0.4, in oxygen atmosphere, but the mechanism has not been explored. Herein, by using first-principles calculations, we attempt to fill this gap by providing atomistic insights into the bonding behaviors of oxygen atom(s) at interfaces constructed by two self-mated diamond (001) or (111) surfaces. The effect of the interfacial oxygen coverage on the optimized interfacial structures is highlighted. The results show that if the oxygen coverage is not higher than 0.5, the two surfaces tend to be connected by oxygen atoms by formation of C—O—C bonds, and thus high friction is expected. Otherwise, the two surfaces keep being separated, and thus low friction is expected. The interfacial electron distributions are manifested to underlie the structural optimizations. Insights gained here together with the findings of T. E. Derry et al. concerning oxygen coverage on diamond surfaces contribute to understanding the unusual frictional behavior of hydrogen-free diamond-like carbons in oxygen atmosphere.

1. Introduction

Friction is a science on the relative motion of two contact surfaces, for which the chemical interactions at the interface play a pivotal role [1—3]. Besides the initial materials in contact with each other [3], the atmosphere usually can affect the chemical nature of the sliding interface and hence the friction outcomes. This claim is well exemplified by the fact that the friction behaviors of various diamond-like carbon (DLC) films are strongly affected by the surrounding atmosphere [4—10]. The participation of environmental gaseous species in friction process is chiefly via tribochemical reaction [4—11]. Hydrogen ambient is known to be important for achieving superlubricity, friction coefficient below 0.01, in DLC films, because hydrogen can chemically bond with the friction-induced carbon dangling bonds and thus H-terminated DLC sliding interface can be maintained [9—11]. The electrostatic repulsion counteracting the weak van der Waals attractions between H-terminated carbon surfaces is claimed to be responsible for the superlubricity [12,13]. In humid air, the hydrogenated surfaces can be destroyed by H_2O and O_2 by creating partial to full OH-terminated surfaces [11,13], and thus hydrogen bonds (i.e., O—H···O) will build across the sliding interface, leading to the friction coefficients of DLC films generally in a range of 0.02—0.2 [14]. The frictional behaviors between H- or OH-terminated carbon surfaces have been intensively verified and interpreted by theoretical simulations as well [9,11,13,15—19].

In contrast, the frictional behavior and mechanism between carbon surfaces that are exclusively bonded with oxygen are scarcely considered. However, this is an important theme, given that oxygen-terminated carbon surfaces are dominant when H-free carbon materials are rubbed in atmospheres where only molecular or atomic oxygen is active. Gharam et al. [8] reported that the H-free DLC film in a dry mixture of O_2 and Ar yielded high friction coefficients with significant fluctuation (0.35 ± 0.05), while in a

* Corresponding author. Key Laboratory of Marine Materials and Related Technologies, Zhejiang Key Laboratory of Marine Materials and Protective Technologies, Ningbo Institute of Materials Technology and Engineering, Chinese Academy of Sciences, Ningbo 315201, China.
E-mail address: lpwang@licp.cas.cn (L. Wang).

humid mixture with 45% RH, the film could show low and steady friction coefficients (0.12 ± 0.01). Similarly, Qi et al. [9] showed that the H-free DLC film produced a high friction coefficient of 0.72 in dry N_2, an intermediate friction coefficient of 0.28 in dry air (O_2:N_2 = 22%:78% and N_2 is inert), and a ultralow friction coefficient of 0.012 in H_2 gas. However, the relatively high friction of the H-free DLC film in dry air has not been explained in the theoretical study because the interaction of O_2 with H-free DLC surface is complex [9]. Recently, Zilibotti et al. [19] paid some attention to one type of O-passivated diamond interface constructed with two oxygenated diamond (001) surfaces with oxygen in ether (C–O–C) configuration. Unfortunately, insights gained from their first-principles study cannot decipher the experimental results reported in refs 8 and 9. They showed that the equilibrium distance between O-terminated diamond surfaces was larger than that between H-terminated diamond surfaces, and the lateral potential energy surface of the oxygenated interface was also smoother than that of hydrogenated one [19]. Therefore, one can expect the oxygenated diamond interface to show a superlow friction coefficient even lower than that of the well-known superlubricating H-passivated interface. However, Feng et al. [20] gave evidence that the atomic O was less effective than atomic H in reducing the friction of a diamond on diamond contact. Then a question is: what is the friction mechanism of H-free diamond-like carbons in molecule or atomic oxygen?

Herein, we aim to uncover the friction mechanism of diamond and H-free DLCs in atmospheres in which oxygen is the sole active species, generating friction coefficients in an unusual range, from 0.2 to 0.4 [8,9,20], for diamond and DLC films [15]. To this end, we preformed first-principles calculations, whose effectiveness for elucidating the frictional mechanism of DLC films has been proved by many researches [3,9,13,15,19]. Insights gained from this study in conjunction with the findings of Derry et al. [21–23] concerning oxygen coverage on diamond surfaces are beneficial for understanding the friction behavior of H-free diamond-like carbons in oxygen atmosphere.

2. Computational details

The first-principles calculations were carried out using the CASTEP code [24], which is a plane-wave pseudopotential method based on density functional theory (DFT). The generalized gradient approximation (GGA) as formulated by Perdew–Burke–Ernzerhof (PBE) was used for the exchange-correlation functional [25]. The electron–ion interactions were treated with Vanderbilt ultrasoft pseudopotentials [26]. All calculations were done with a 380 eV cutoff energy and a 10 × 5 × 1 Monkhorst–Pack [27] grid generating 25 irreducible k-points. The Broyden–-Fletcher–Goldfarb–Shanno (BFGS) algorithm [28] with line search was used for geometry optimizations. Convergence thresholds were set to 5×10^{-6} eV/atom for the total energy, 5×10^{-4} Å for the maximum displacement, 0.01 eV/Å for the maximum force, and 0.02 GPa for the stress on the cell.

Diamond (001) and (111) surfaces with 12 layers of carbon atoms were cleaved from a optimized diamond crystal whose lattice constant is 3.568 Å (the experimental data is 3.567 Å). The thickness of slabs had been proved to be large enough to simulate the semi-infinite bulk [19]. The surfaces were modeled by (2 × 1) supercells, as illustrated in Fig. 1. The interfaces were constructed with two same diamond surface slabs with mirror-symmetry. Thus, the interface models had totally 48 carbon atoms, of which 4 atoms had dangling bonds at the interfaces. Various numbers of oxygen atoms from 1 to 4 were added in the interface regions to take into account the effect of coverage. In fact, oxygen molecules would dissociate into atoms and bond to carbon atoms during the relaxation. Considering the limited adsorption configurations of oxygen on diamond surfaces, we could firstly distribute the oxygen atom(s) to the two surfaces and move it (them) close to the adsorption site(s), and then optimize the interfacial models. Two types of interfaces could be obtained, depending on the distance between the two surfaces and the number of oxygen atoms. If the two surfaces were apparently separated from each other in the optimized interface (type I), we would narrow the separation between the two surfaces to determine whether or not the interface could be sutured by oxygen atoms (type II). Interactions between periodic replicas of interface models were minimized by including a vacuum region of 15 Å. During geometry optimization, all atoms were allowed to fully relax while the cell parameters were fixed. Moreover, differential electron density and Mulliken atomic population were calculated to detect the mechanisms behind the phenomena observed in structural optimizations.

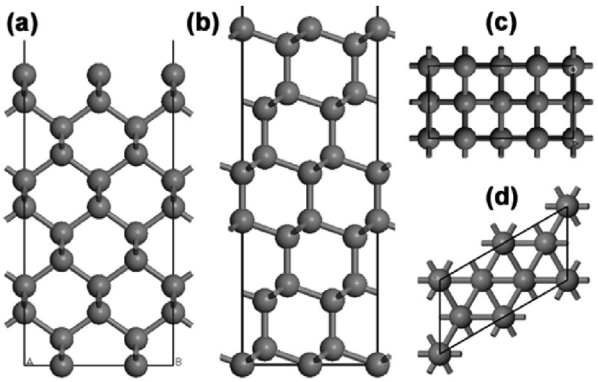

Fig. 1. Periodic models of diamond (001) and (111) surfaces used to build interfaces: (a) the (001) surface, (b) the (111) surface, (c) top view of the (001) surface, and (d) top view of the (111) surface.

3. Results and discussion

3.1. Structural geometry and energetic stability

Fig. 2 presents the optimized structures for one oxygen atom adsorbed at the diamond (001) interface, i.e., the interface constructed by two self-mated diamond (001) surfaces. To simplify the expression, we use the serial number of a figure to stand for the structure showed in that figure, for example, '2a' to denote the structure in Fig. 2a. The oxygen atom can either bond with one carbon atom (2a) or two carbon atoms (2c) on one diamond (001) surface. In the former case, the C–O bond length (BL) is 1.314 Å, which is longer than the BL of C=O (1.22 Å) in ketone but shorter than the BL of C–O (1.36 Å) in ester. Besides, there is a C–C bond with BL of 1.633 Å, longer than the BL of C–C single bond in bulk diamond (1.545 Å), linking to the carbon atom in the C–O bond. In the latter one, a C–O–C bond with BL of 1.422 Å and bond angle (BA) of 107.6° is formed. The other diamond (001) surface will reconstruct itself to form dimers along the [110] direction. The BLs of carbon dimers (1.393 and 1.396 Å) are shorter than that of standard C–C single bond in bulk diamond, indicating the presence of C=C double bonds within the dimmers [19]. If we narrow the distance between the two surfaces, the two slabs will be bonded together by C–O–C and C–C bonds, and the total energies of the interfacial systems decrease significantly by ~3.5 eV (Table 1).

One oxygen atom can only bond with one carbon atom on the diamond (111) surface (Fig. 3). In fact, the oxygen atom will spontaneously move from the bridge site to a site close to the on-top site during the optimization process [23]. The distance between the

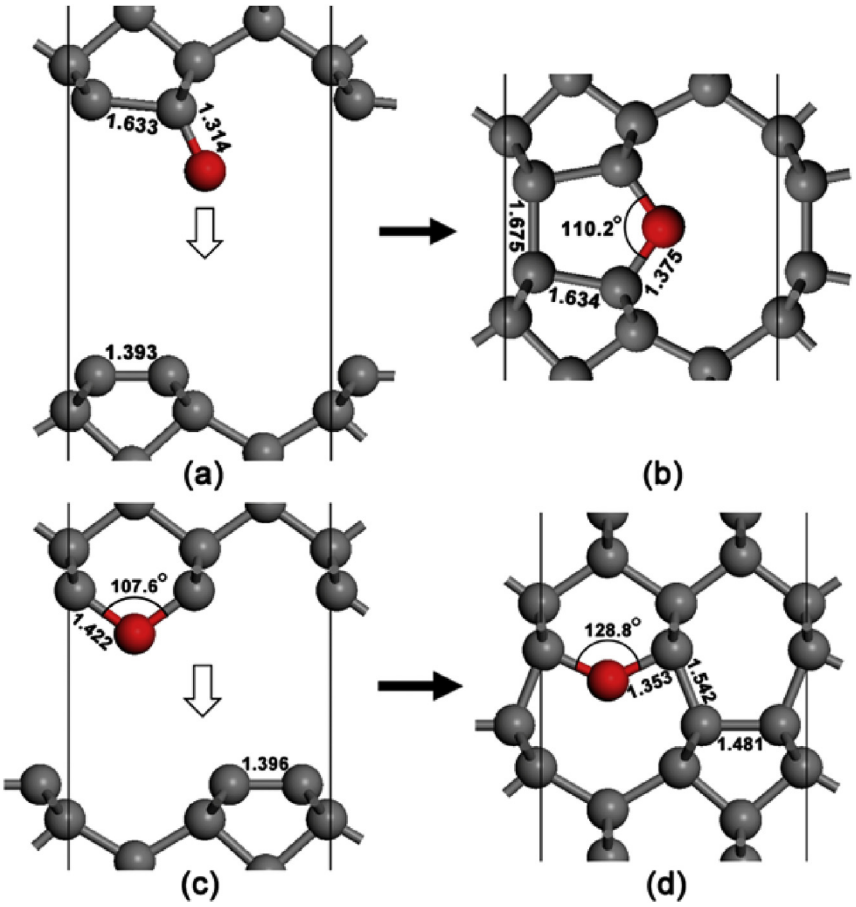

Fig. 2. Optimized structures for one oxygen atom adsorbed at the diamond (001) interface. The bond lengths are given in Å, angles are in degrees. The downward hollow arrow indicates narrowing the distance between the two slabs. The rightward black arrow represents the structural transformation from left to right, for example from 2a to 2b. Carbon and oxygen atoms are shown as gray and red spheres, respectively. (A colour version of this figure can be viewed online.)

Table 1
Calculated energy in eV for the optimized interfacial structures.

1 oxygen atom		2 oxygen atoms		3 oxygen atoms		4 oxygen atoms	
Structure	Energy	Structure	Energy	Structure	Energy	Structure	Energy
2a	−7859.05	4a	−8296.68	9a	−8732.96	9c	−9171.02
2b	−7862.93	4b	−8299.30	9b	−8733.68	9d	−9169.66
2c	−7859.18	5a	−8294.83				
2d	−7862.67	5b	−8294.57				
3a	−7861.62	6a	−8295.23				
3b	−7863.19	6b	−8295.22				
		6c	−8297.07				
		7a	−8297.65				
		7b	−8299.97				
		8a	−8297.71				
		8b	−8297.72				

carbon and oxygen atom is 1.332 Å, hinting a C—O single bond formed between them. If the two slabs are placed closer, the oxygen atom will bond with the opposite carbon atom and a C—O—C bond with BL of 1.371 Å and BA of 153.5° will be formed, releasing total energy of 1.57 eV (Table 1).

If we put two oxygen atoms at the diamond (001) interface, six structures (i.e., 4a, 4b, 5a, 6a, 6b, and 6c) could be obtained. The geometric parameters, BLs and BAs, are indicated in the corresponding structures. Except 4b, in which the two diamond (001) surfaces are connected by two oxygen atoms in ether configuration and a hexatomic ring is formed, the other interfaces all belong to type I. Yet, 4b has the lowest energy, hinting it is the most thermodynamically stable one. Structural transformations are also found in them, as shown in Figs. 4 and 5. The 4a → 4b transformation releases energy of 2.62 eV (Table 1). As for 5a, straightforward narrowing the separation will lead to the formation of a peroxy bond and the length of O—O bond is 1.485 Å (not shown here), but the transformation causes the increase of system energy by 0.48 eV, indicating this process is unfavorable. If we firstly make lateral movement between the two surfaces (5a → 5b, simulating the shearing in friction) and then narrow the separation, favorable structural transformation, system energy reducing by 4.73 eV, will

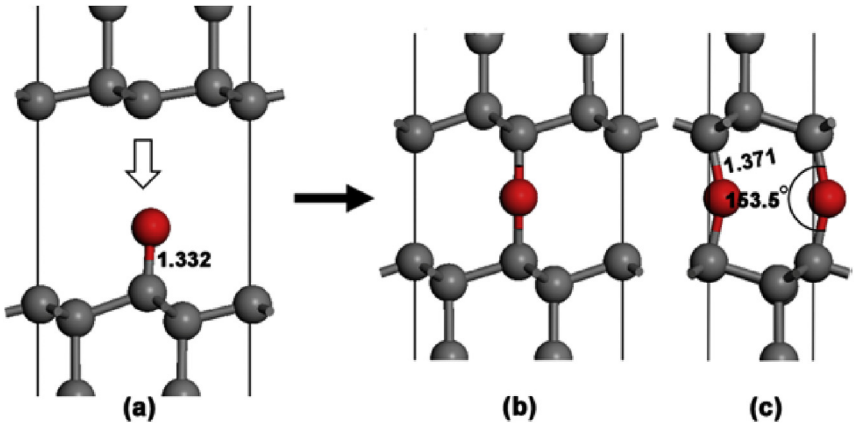

Fig. 3. Optimized structures for one oxygen atom adsorbed at the diamond (111) interface. The (c) is the side view of (b). Other instructions for understanding this figure can be found in the legend of Fig. 2. (A colour version of this figure can be viewed online.)

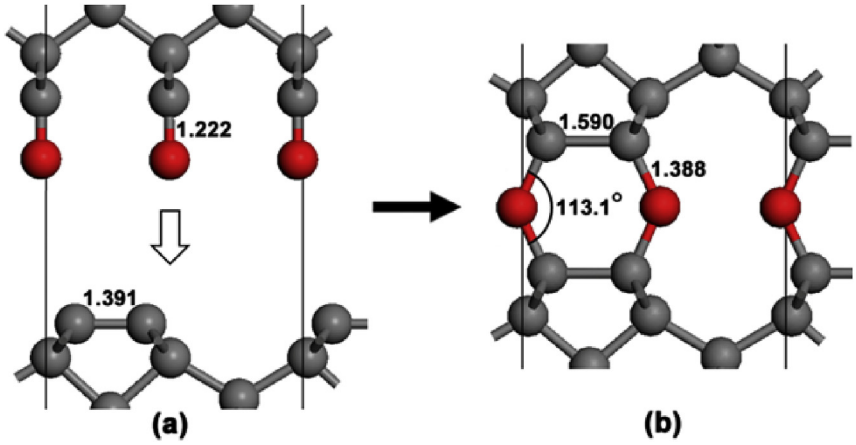

Fig. 4. Structural transformation for two oxygen atoms adsorbed on the same side of the diamond (001) interface in ketone configuration. (A colour version of this figure can be viewed online.)

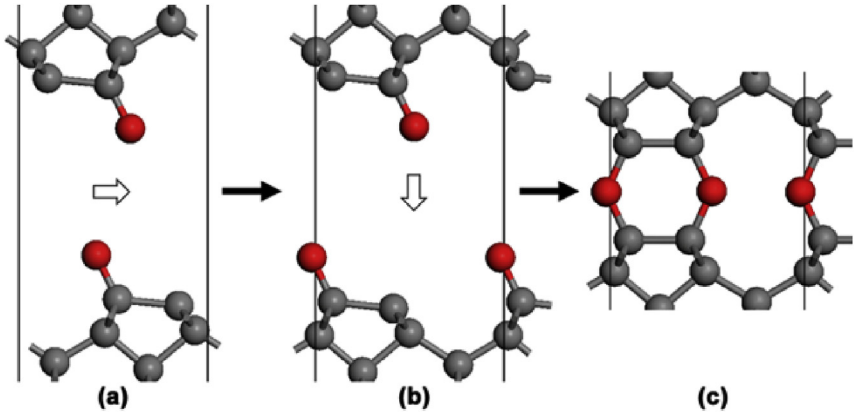

Fig. 5. Structural transformation for two oxygen atoms adsorbed on the two sides of the diamond (001) interface. The rightward hollow arrow indicates the lateral movement of the two slabs. (A colour version of this figure can be viewed online.)

happen. The lateral movement process results in a slight increase of system energy by 0.26 eV, hinting the low shearing resistance between the two surfaces. The type I interfaces with two oxygen atoms in ether configuration (Fig. 6) cannot transform to type II ones.

There are only three structures for two oxygen atoms adsorbed at the diamond (111) interface, i.e., 7a, 7b and 8a. Among them, 7b is a type II interface and has the lowest energy; hence it is the most thermodynamically stable one. Structural transformations among them are shown in Figs. 7 and 8, both of which release of total energy of ~2.3 eV (Table 1). Like in the diamond (001) interface, a peroxy bond can also be formed by narrowing the interface

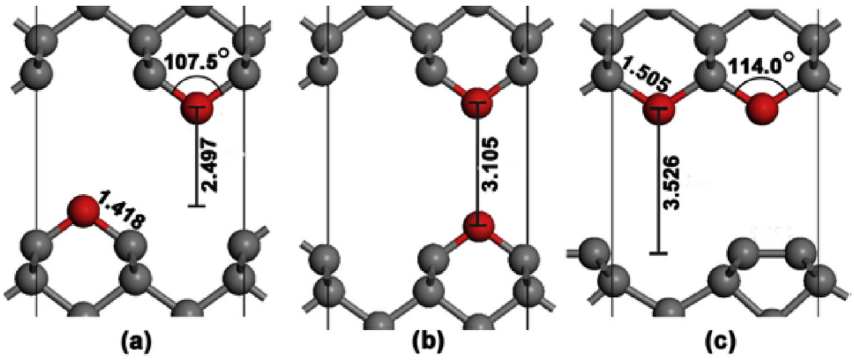

Fig. 6. Optimized type I interface structures for two oxygen atoms adsorbed at the diamond (001) interface in ether configuration. (A colour version of this figure can be viewed online.)

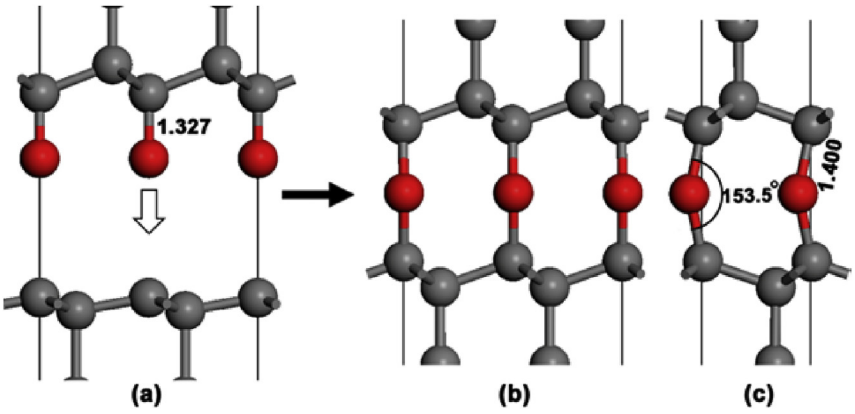

Fig. 7. Structural transformation for two oxygen atoms adsorbed on the same side of the diamond (111) interface. The (c) is the side view of (b). (A colour version of this figure can be viewed online.)

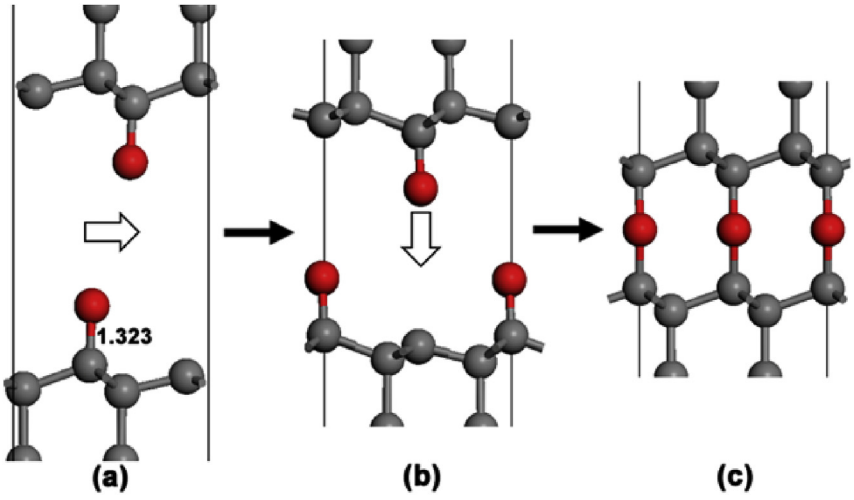

Fig. 8. Structural transformation for two oxygen atoms adsorbed on two sides of the diamond (111) interface. (A colour version of this figure can be viewed online.)

distance in 8a, but the process is energy unfavorable by 0.48 eV. Relative lateral movement is also required for the structural transformation, as shown in Fig. 8.

There are totally nine interface structures for three and four oxygen atoms adsorbed at the diamond (001) and (111) interfaces, but all they are belong to the type II interface. Fig. 9 gives four representative examples. If we narrow the separations in them, the mated surfaces will automatically be away from each other, indicating the repulsive force. The well-separated interface signifies the low interfacial shear strength and friction [19].

3.2. *Differential electron density and Mulliken charge analysis*

To detect the mechanisms underlying the structural

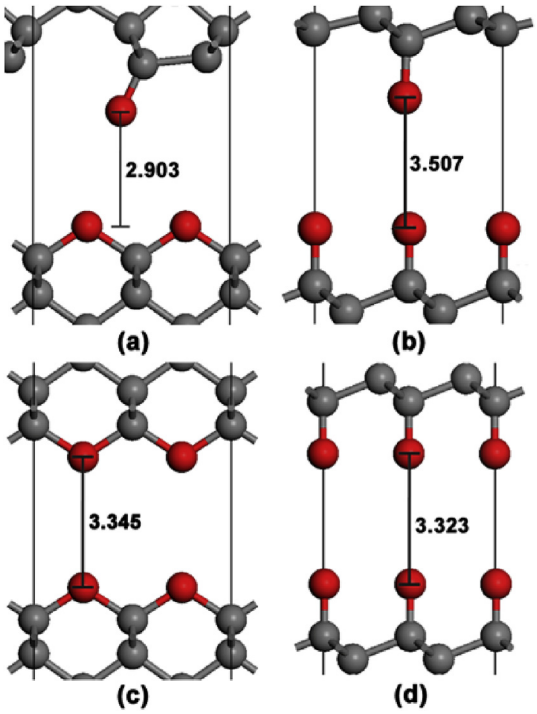

Fig. 9. Examples of optimized structures for (a, b) three oxygen atoms and (c, d) four oxygen atoms adsorbed at (a, c) the diamond (001) interface and (b, d) the diamond (111) interface. (A colour version of this figure can be viewed online.)

optimizations, we calculate the differential electron density and the Mulliken atomic population. The planar differential electron density maps for the structural transformations 5b → 5c and 7a → 7b are shown in Figs. 10 and 11, respectively, and the Mulliken atomic charges are also shown. The C—O bonds are polarized with oxygen atoms bearing negative charges and carbon atoms positive charges, following the difference in electronegativity between the C (2.55) and O (3.44) atoms. The carbon atoms across from oxygen atoms are also slightly positively charged. Moreover, the increment of net charge on oxygen atom is equal to that on its opposite carbon atom during the narrowing of interface gap, indicating a cross-interface charge-transfer behavior. Hence, the attraction between the oxygen atom and the carbon atom, which makes the two surfaces close to each other, increases enormously. Finally, the two surfaces are bonded together by formation of cross-interface C—O—C bonds.

There are two contributions to the electrostatic repulsion between O-terminated diamond surfaces, as depicted in Fig. 12. One is the difference in electronegativity between the C and O atoms, resulting in oxygen atoms bearing like negative charges. The other is the lone-pairs on oxygen atoms since lone-pairs repel mutually. The latter does not present in the H-passivated carbon interface, since hydrogen atom has no lone-pair on it. Owing to such electrostatic repulsions, the two O-terminated diamond surfaces keep to be well-separated.

3.3. The frictional mechanism of H-free diamond-like carbons in oxygen atmosphere and its implications

Our results showed that when the oxygen coverage is not higher than 0.5 the diamond interfaces are tend to be sutured by oxygen by formation of C—O—C bonds and thus high-friction is expected, and further increase of the oxygen coverage will cause electrostatic repulsions at the interfaces and thus low-friction is expected. Yet, these findings are seemingly incompatible with the relatively high friction coefficients of H-free carbons in atmospheres where oxygen is abundant [8,9,20]. This concern can be dispelled by the findings of Derry and coworkers [21—23] concerning the oxygen coverage on diamond surfaces. They measured the oxygen coverage on natural diamond surfaces by X-ray photoelectron spectroscopy and Rutherford backscattering spectrometry, and the results unexpectedly showed that the coverage of chemisorbed oxygen on diamond (001) and (111) surfaces is only about 1/2 and 1/3 monolayer, respectively [21,22]. The underlying reason is the fact that the van der Waals diameter of oxygen atom (2.80 Å) is larger than the nearest distance between two active carbon atoms on the diamond surfaces (2.54 Å), which can result in the steric hindrance that prevents the accommodation of oxygen at the adjacent sites and limits the oxygen coverage to partial monolayer, as illustrated in Fig. 13. The notion was further consolidated by their subsequent DFT study [23], where they demonstrated that increasing oxygen coverage higher than 1/3 monolayer on the diamond (111) surface will develop repulsive interactions between oxygen atoms.

Despite not regular as the diamond surfaces, the surfaces of H-free DLCs probably also cannot be completely terminated by oxygen due to the same reason. As a consequence, some cross-interface C—O—C bonds can be formed with the aid of the applied normal load. In other atomic-domains of the friction interface, electrostatic repulsions between oxygen atoms bonding with carbon atoms are present simultaneously. The coexistence of the two types of interfacial interactions will give rise to the intermediate frictional outcomes.

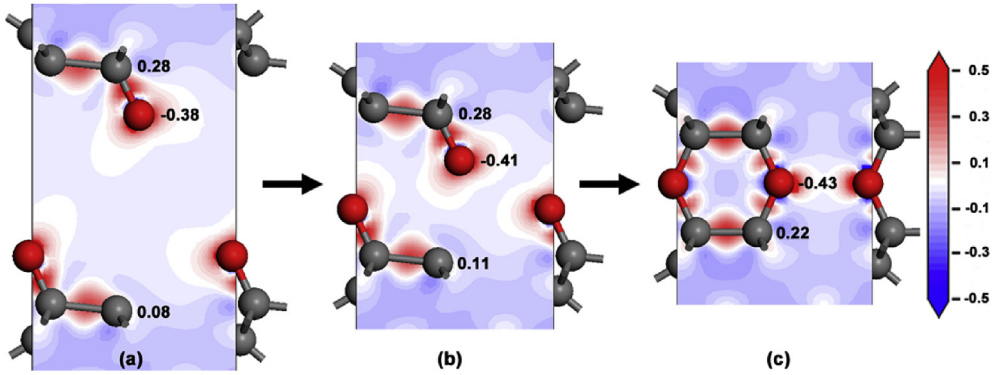

Fig. 10. Differential electron density maps for the structural transformation from 5b to 5c with a slice through the centers of the atoms. The Mulliken charges are marked at the right sides of the corresponding atoms in electron/atom. There are 32 contour levels plotted with blue corresponding to −0.5 and red to 0.5 e/Å^3, as indicated in the scale bar. (A colour version of this figure can be viewed online.)

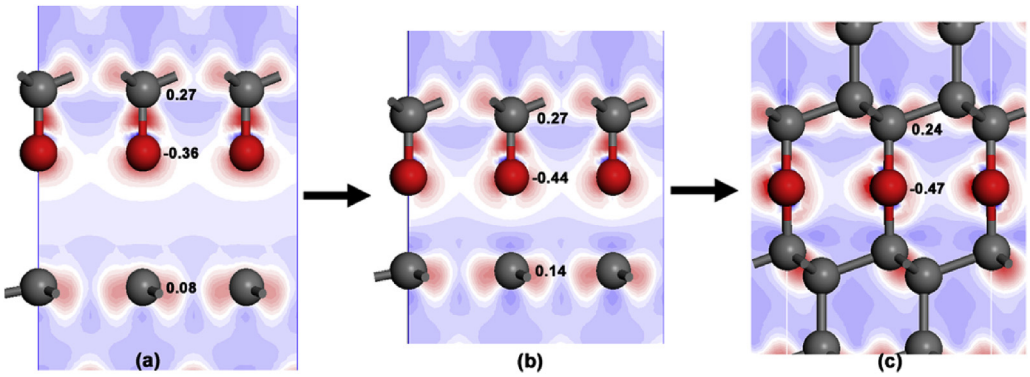

Fig. 11. Differential electron density maps for the structural transformation from 7a to 7b. Instructions for understanding this figure are the same as for Fig. 10. (A colour version of this figure can be viewed online.)

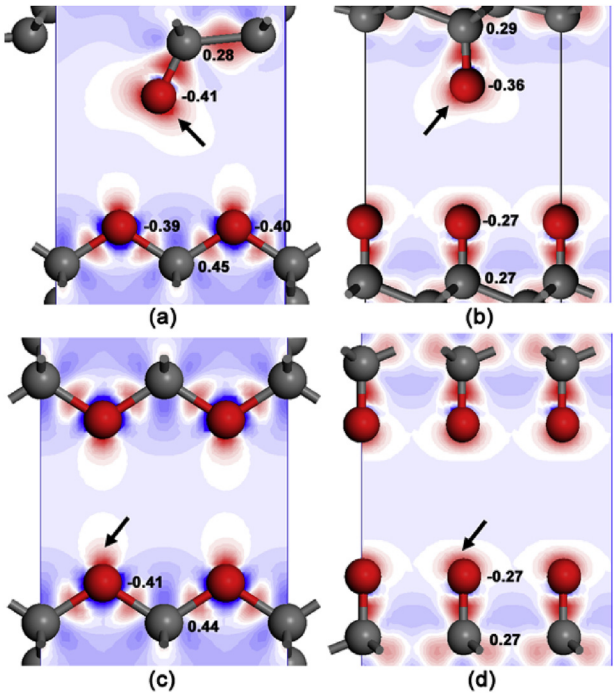

Fig. 12. Differential electron density maps for the structures presented in Fig. 9. The black arrows point to the concentration of electron density, indicating the present of lone-pairs on the surfaces. (A colour version of this figure can be viewed online.)

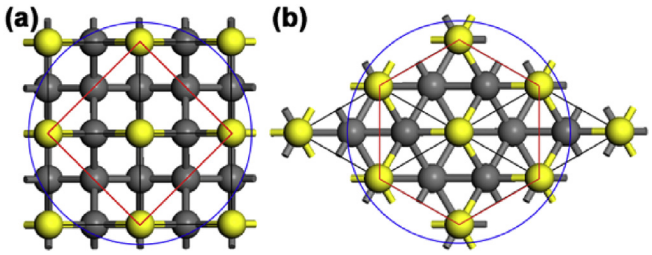

Fig. 13. Schematics to explain the findings of Derry et al. [21,22] that the chemisorbed oxygen coverage is ~1/2 monolayer on the diamond (001) surface and ~1/3 monolayer on the (111) surface. Top views of the (2 × 2) unit cell for (a) the diamond (001) surface and (b) the diamond (111) surface. The carbon atoms at the surfaces are in yellow. The nearest surface atoms around one active atom are connected by red lines. The blue circle represents the van der Waals diameter of oxygen atom. The nearest distance between the surface atoms is 2.54 Å and the van der Waals diameter of oxygen atom is 2.80 Å. The zone surrounded by red lines contains two surface carbon atoms for the diamond (001) surface and three for the (111) surface. When one oxygen atom adsorbs on the centric carbon atom, the surrounding sites are blocked, explaining the findings that the chemisorbed oxygen coverage is only ~1/2 monolayer on diamond (001) surface and ~1/3 monolayer on (111) surface. (A colour version of this figure can be viewed online.)

The mechanism proposed here is also relevant for studies in which H-free carbons are rubbed under a low humidity condition with a high contact stress, because O-terminated domains can originate from the further decomposition of adsorbed hydroxyl fragments. Konicek et al. [29] have shown an noticeable increase of C—O bonds on the wear surfaces of H-free carbons, compared with the unworn surfaces that are passivated by dissociated water molecules, especially under low humidity and high load conditions. The decomposition of C—OH groups confined between two diamond surfaces into C—O groups has been further confirmed by Zilibotti et al. by large scale *ab initio* molecular dynamics [30].

Besides, the friction-reduction of a hydrogenated DLC film enabled by introducing of oxygen gas with pressure of 10 Pa into a high-vacuum chamber as reported by Fontaine et al. [31] can be understood now. The C—H bonds at the rubbing interface can be broken by frictional force and the exposed carbon dangling bonds can be terminated by chemisorbed oxygen atoms. Yet, the density of friction-induced dangling bonds must be quite low for hydrogenated DLC films at the very beginning of sliding [32], which allows the dangling bonds to be sufficiently terminated by oxygen atoms because in this case, a carbon dangling bond will be surrounded by C—H bonds, the steric hindrance for oxygen adsorption is small if any. Therefore, the friction coefficients can maintain low (around 0.02). Otherwise, with the accumulation of carbon dangling bonds at the rubbing interface, high-friction is inevitable.

Finally, we would like to discuss the implications for better understanding the low-friction mechanisms of the H- and the OH-terminated carbon surfaces. The small van der Waals diameter of hydrogen atom (2.2—2.4 Å) allows the carbon surfaces to be fully passivated. That is to say that the small size of hydrogen also is one of essential reasons for the superlubricity of DLC films in H_2 gas. The OH-terminated carbon surfaces can be viewed as H-passivated C—O surfaces; therefore, the low-friction behaviors of various carbons in humid conditions can be ascribed to the passivation of hydrogen as well.

4. Conclusions

The friction mechanism of H-free carbon materials including diamond and H-free DLCs in oxygen atmosphere, where their friction coefficients are reported to be in an intermediate range

from 0.2 to 0.4, is explored by using first-principles calculations. The carbon to carbon frictional interfaces are modeled by self-mated diamond (001) and (111) surfaces, and 1 to 4 oxygen atoms are placed in the interface regions, and then structural optimizations are conducted. The results show that if the interfacial oxygen coverage is not higher than 0.5, the mating surfaces tend to be connected by oxygen atoms by formation of C—O—C bonds, and thus high-friction is expected. Otherwise, the two surfaces keep being separated, and thus low-friction is expected. The interfacial electron distributions are manifested to underlie the structural optimizations. According to the insights gained here together with the findings of T. E. Derry et al. concerning oxygen coverage on diamond surfaces, we suggest that it is the coexistence of high-friction atomic domains and low-friction domains at the friction interface that leads to the intermediate friction coefficients of hydrogen-free diamond-like carbons in oxygen atmosphere.

Acknowledgment

The authors gratefully acknowledged financial support provided by the National Key Basic Research Program (No. 2014CB643302) and National Natural Science Foundation of China (Grant No. 51322508).

References

[1] H. Gao, A. Otero-de-la-Roza, S.M. Aouadi, A. Martini, E.R. Johnson, Chemical basis of the tribological properties of $AgTaO_3$ crystal surfaces, J. Phys. Chem. C 118 (2014) 17577—17584.

[2] J.D. Schall, G. Gao, J.A. Harrison, Effects of adhesion and transfer film formation on the tribology of self-mated DLC contacts, J. Phys. Chem. C 114 (2010) 5321—5330.

[3] L. Cui, Z. Lu, L. Wang, Toward low friction in high vacuum for hydrogenated diamond like carbon by tailoring sliding interface, ACS Appl. Mater. Interfaces 5 (2013) 5889—5893.

[4] L. Cui, Z. Lu, L. Wang, Probing the low-friction mechanism of diamond-like carbon by varying of sliding velocity and vacuum pressure, Carbon 66 (2014) 259—266.

[5] X. Chen, T. Kato, M. Nosaka, Origin of superlubricity in a-C: H:Si films: a relation to film bonding structure and environmental molecular characteristic, ACS Appl. Mater. Interfaces 6 (2014) 13389—13405.

[6] L. Cui, Z. Lu, L. Wang, Environmental effect on the load-dependent friction behavior of a diamond-like carbon film, Tribol. Int. 82 (2015) 195—199.

[7] K.D. Koshigan, F. Mangolini, J.B. McClimon, B. Vacher, S. Bec, R.W. Carpick, J. Fontaine, Understanding the hydrogen and oxygen gas pressure dependence of the tribological properties of silicon oxide-doped hydrogenated amorphous carbon coatings, Carbon 93 (2015) 851—860.

[8] A.A. Gharam, M.J. Lukitsch, Y. Qi, A.T. Alpas, Role of oxygen and humidity on the tribo-chemical behaviour of non-hydrogenated diamond-like carbon coatings, Wear 271 (2011) 2157—2163.

[9] Y. Qi, E. Konca, A.T. Alpas, Atmospheric effects on the adhesion and friction between non-hydrogenated diamond-like carbon (DLC) coating and aluminum—a first principles investigation, Surf. Sci. 600 (2006) 2955—2965.

[10] J. Fontaine, M. Belin, T. Le Mogne, A. Grill, How to restore superlow friction of DLC: the healing effect of hydrogen gas, Tribol. Int. 37 (2004) 869—877.

[11] H. Guo, Y. Qi, Environmental conditions to achieve low adhesion and low friction on diamond surfaces, Model. Simul. Mater. Sci. Eng. 18 (2010) 034008.

[12] A. Erdemir, The role of hydrogen in tribological properties of diamond-like carbon films, Surf. Coat. Technol. 146—147 (2001) 292—297.

[13] S. Dag, S. Ciraci, Atomic scale study of superlow friction between hydrogenated diamond surfaces, Phys. Rev. B 70 (2004), 241401(R).

[14] A. Erdemir, C. Donnet, Tribology of diamond-like carbon films: recent progress and future prospects, J. Phys. D Appl. Phys. 39 (2006) R311—R327.

[15] G. Zilibotti, M.C. Righi, Ab initio calculation of the adhesion and ideal shear strength of planar diamond interfaces with different atomic structure and hydrogen coverage, Langmuir 27 (2011) 6862—6867.

[16] J.M. Martin, M.I.D.B. Bouchet, C. Matta, Q. Zhang, W.A. Goddard III, S. Okuda, T. Sagawa, Gas-phase lubrication of ta-C by glycerol and hydrogen peroxide. Experimental and computer modeling, J. Phys. Chem. C 114 (2010) 5003—5011.

[17] M.I. De Barros Bouchet, G. Zilibotti, C. Matta, M.C. Righi, L. Vandenbulcke, B. Vacher, J.M. Martin, Friction of diamond in the presence of water vapor and hydrogen gas. Coupling gas-phase lubrication and first-principles studies, J. Phys. Chem. C 116 (2012) 6966—6972.

[18] Y. Morita, T. Shibata, T. Onodera, R. Sahnoun, M. Koyama, H. Tsuboi, N. Hatakeyama, A. Endou, H. Takaba, M. Kubo, et al., Effect of surface termination on superlow friction of diamond film: a theoretical study, Jpn. J. Appl. Phys. 47 (2008) 3032—3035.

[19] G. Zilibotti, M.C. Righi, M. Ferrario, Ab initio study on the surface chemistry and nanotribological properties of passivated diamond surfaces, Phys. Rev. B 79 (2009) 075420.

[20] Z. Feng, Y. Tzeng, J.E. Field, Friction of diamond on diamond in ultra-high vacuum and low-pressure environments, J. Phys. D Appl. Phys. 25 (1992) 1418—1424.

[21] J.O. Hansen, R.G. Copperthwaite, T.E. Derry, J.M. Pratt, A tensiometric study of diamond (111) and (110) faces, J. Colloid Interface Sci. 130 (1989) 347—358.

[22] D.B. Rebuli, T.E. Derry, E. Sideras-Haddad, B.P. Doyle, R.D. Maclear, S.H. Connell, J.P.F. Sellschop, Oxygen on diamond surfaces, Diam. Relat. Mater. 8 (1999) 1620—1622.

[23] T.E. Derry, N.W. Makau, C. Stampfl, Oxygen adsorption on the (1×1) and (2×1) reconstructed C(111) Surfaces: a density functional theory study, J. Phys. Condens. Matter 22 (2010) 265007.

[24] S.J. Clark, M.D. Segall, C.J. Pickard, P.J. Hasnip, M.J. Probert, K. Refson, M.C. Payne, First principles methods using CASTEP, Z. Kristallogr. 220 (2005) 567—570.

[25] J.P. Perdew, K. Burke, M. Ernzerhof, Generalized gradient approximation made simple, Phys. Rev. Lett. 77 (1996) 3865—3868.

[26] D. Vanderbilt, Soft self-consistent pseudopotentials in a generalized eigenvalue formalism, Phys. Rev. B 41 (1990) 7892—7895.

[27] H.J. Monkhorst, J.D. Pack, Special points for brillouin-zone integrations, Phys. Rev. B 13 (1976) 5188—5192.

[28] B.G. Pfrommer, M. Côté, S.G. Louie, M.L. Cohen, Relaxation of crystals with the quasi-newton method, J. Comput. Phys. 131 (1997) 233—240.

[29] A.R. Konicek, D.S. Grierson, A.V. Sumant, T.A. Friedmann, J.P. Sullivan, P.U.P.A. Gilbert, W.G. Sawyer, R.W. Carpick, Influence of surface passivation on the friction and wear behavior of ultrananocrystalline diamond and tetrahedral amorphous carbon thin films, Phys. Rev. B 85 (2012) 155448.

[30] G. Zilibotti, S. Corni, M.C. Righi, Load-induced confinement activates diamond lubrication by water, Phys. Rev. Lett. 111 (2013) 146101.

[31] J. Fontaine, T. Le Mogne, J.L. Loubet, M. Belin, Achieving superlow friction with hydrogenated amorphous carbon: some key requirements, Thin Solid Films 482 (2005) 99—108.

[32] K. Hayashi, K. Tezuka, N. Ozawa, T. Shimazaki, K. Adachi, M. Kubo, Tribochemical reaction dynamics simulation of hydrogen on a diamond-like carbon surface based on tight-binding quantum chemical molecular dynamics, J. Phys. Chem. C 115 (2011) 22981—22986.